Geofísica Internacional (2025) **64-2**: 1577- 1592

Water exchange between the Gulf of California and the Pacific Ocean: results from a one-year global HYCOM simulation

Gonzalo Acosta-Solís[1], Manuel López-Mariscal[1] and Luis Zamudio[2]

Abstract

The mean and seasonal water exchange between the Gulf of California and the Pacific Ocean (PO) are analyzed with a one-year global HYCOM simulation. At the mouth of the gulf there are six alternating layers of inflow and outflow of mean transport with inflow in the uppermost layer (0-68 m) and the largest outflow in the second layer (68-198 m). The three uppermost layers have the largest mean transports, and they can be identified more than two thirds along the length of the gulf with approximately the same thickness. The difference in the transport between the interior of the gulf and the transport at the mouth in the upper layer, shows that there must be an upward mean transport (upwelling) into the upper layer along almost the entire length of the gulf. The two deepest layers have smaller mean transports, but the deepest layer has an outflow that is about half of the inflow of the surface layer implying a very large vertical transport into that layer. We obtained the seasonal exchange by fitting annual and semiannual harmonics to the monthly mean transports in each layer. The maxima and minima of the seasonal exchange are larger than the mean and they occur in summer and autumn showing that most of the exchange with the PO occurs during those two seasons. The maximum inflow (~ 0.8 Sv, 1 Sv = 1×10^6 m^3/s) in the upper layer occurs at the beginning of July and the maximum outflow at the beginning of November (~ 0.4 Sv). The transport in the second layer is out of the gulf all year round. The fourth layer (380-822 m) has the smallest mean transport of all layers but, together with the first layer, has the largest seasonal transport. The net outflowing transport is about 0.2972 Sv, which gives a turnover time of approximately 14 years for the gulf.

Key words: Gulf of California, exchange with the Pacific Ocean, seasonal variations, turnover time.

Resumen

Se analiza el intercambio medio y estacional entre el Golfo de California y el Océano Pacífico (OP) utilizando una simulación anual del modelo global HYCOM. En la boca del golfo se encontraron seis capas que alternan entre transporte medio de entrada y salida, con flujo de entrada en la capa superficial (0-68 m) y de salida en la segunda capa (68-198 m). Las tres capas superiores tienen los transportes más grandes y se pueden identificar más de dos tercios de la longitud del golfo con un espesor aproximadamente constante. La diferencia en el transporte superficial entre el interior del golfo y el de la boca, muestra que existe un transporte vertical medio hacia arriba (surgencia) hacia la capa superficial en casi toda la longitud del golfo. Las dos capas más profundas tienen transportes más pequeños, pero la más profunda tiene un transporte hacia afuera que es aproximadamente la mitad del transporte entrando por la capa superficial, lo cual implica que hay un transporte vertical intenso hacia esa capa. Obtuvimos el intercambio estacional ajustando armónicos anuales y semianuales a los promedios mensuales del transporte en cada capa. Los máximos y mínimos del intercambio estacional son más grandes que la media, y los valores extremos más grandes ocurren en verano y otoño, mostrando que durante esos periodos se da el intercambio más fuerte con el OP. El transporte de entrada máximo (~ 0.8 Sv, 1 Sv = 1×10^6 m^3/s) en la capa superficial ocurre a principios de julio, y el máximo de salida a principios de noviembre (~ 0.4 Sv). El transporte en la segunda capa es de salida durante todo el año. El transporte medio en la cuarta capa es el más pequeño, pero junto con la primera capa, tiene los transportes estacionales más grandes. El transporte neto de salida son 0.2972 Sv, lo cual da un tiempo de residencia del agua del golfo de aproximadamente 14 años.

Palabras clave: Golfo de California, intercambio con el Océano Pacífico, variaciones estacionales, tiempo de residencia.

Received: July 29, 2024; Accepted: January 23, 2024; Published on-line: April 1, 2025.

Editorial responsibility: Dr. José Gómez Valdés

* Corresponding author: Manuel López-Mariscal, malope@cicese.mx
[1] CICESE, Depto. de Oceangrafía Física, Ensenada, Baja California, México.
[2] Florida State University, Center for Oceanic-Atmospheric Prediction Studies, Tallahassee, Florida, USA.

Gonzalo Acosta-Solís, Manuel López-Mariscal, Luis Zamudio

https://doi.org/10.22201/igeof.2954436xe.2025.64.2.1815

1. Introduction

It has long been recognized that the Pacific Ocean (OP) exerts an important dynamical and thermodynamical influence in the Gulf of California (GC), ranging in time scales from the tides to the interannual (e.g., Baumgartner and Christensen, 1985; Marinone, 1997; Ripa, 1997; Lavín and Marinone, 2003). The gulf is an evaporative basin which losses, on average, about 1 m of water per year through the surface (Castro *et al.*, 1994; Berón-Vera and Ripa, 2000), which implies an average, net incoming transport of about 5×10^{-3} Sv (1 Sv = 1×10^6 m^3/s). However, unlike the Mediterranean and Red Seas, the gulf gains heat through the surface (Bray, 1988), and this has prompted the idea that the gulf may have an estuarine-like circulation with outflow in a surface layer and inflow in a layer below, with a near-surface seasonally reversing layer (Bray, 1988; Lavín and Marinone, 2003). But the gulf has no sill at its mouth, and therefore it has an unrestricted exchange with the PO. This unrestricted communication with the PO, together with the complex circulation around its mouth (Kessler, 2006; Portela *et al.*, 2016) and the equatorial influence via coastally-trapped waves (Gómez-Valdivía, *et al.*, 2015) points to a more complex exchange between the gulf and the PO.

Flow at the mouth of the gulf has been studied mainly using hydrographic observations and associated geostrophic velocities (e.g., Mascarenhas *et al.*, 2004; Castro *et al.*, 2006; Castro *et al.*, 2017; Collins and Castro, 2022). Mascarenhas *et al.* (2004) were the first to calculate a mean geostrophic section across the gulf's mouth and they found a broad region of inflow along the Sinaloa (mainland) coast and outflow along de Baja California (BC) coast, with two narrower bands of alternating flow between the broader regions of inflow and outflow adjacent to the coasts. Recently, Collins and Castro (2022) using more observations, calculated the mean geostrophic currents at the mouth. They found the same general pattern of cyclonic flow, but without the mid-sections of inflow and outflow bands. Their mean section was, roughly, evenly divided between inflow to the east and outflow to the west. They also calculated the laterally integrated transport across the mouth of the gulf and found a mean inflowing layer in the upper 150 m and an outflowing layer below down to 400 m. Zamudio *et al.* (2008) calculated mean, and monthly mean meridional velocities at the mouth of the gulf using HYbrid Coordinate Ocean Model (HYCOM) simulations but no integrated transports across the mouth were reported. The mean meridional velocities did capture the general cyclonic pattern with inflow through the east and outflow to the west.

Despite these very important observational and modelling efforts there has been no articles reporting the vertical structure of the mean volume exchange with the PO throughout the water column at the mouth of the gulf. Moreover, we do not know what the seasonal variation of this exchange, nor the along-gulf structure of the volume transport is. In this article we give a description of the mean and seasonal exchange of the gulf with the PO; and also look into the along-gulf structure of the volume transport using a one-year, global simulation of the HYCOM. One important advantage of using a global simulation is that it includes the phenomena of the eastern tropical Pacific which influence the exchange with the gulf. In the next section we give a brief description of the model; in section three we describe the results; and in section four we discuss the results and give concluding remarks.

2. The HYCOM simulation, and methods

The HYCOM is a hydrostatic ocean model which, as its name indicates, employs a hybrid vertical coordinate system. The model uses isopycnic (density tracking) coordinates in most of the open stratified ocean, but switches to z-coordinates (fixed water depths) in the upper mixed layer. It also uses sigma (terrain following) coordinates in shallow regions. The model has been extensively used by the ocean modelling community and a fuller description can be found in Zamudio *et al.* (2008) and references therein. In this article we use a one-year simulation known as expt_06.1, which is forced at the surface with hourly heat fluxes and wind stress from the atmospheric Navy Global Environmental Model (NAVGEM). The model also includes tidal forcing by the five largest constituents (M_2, S_2, N_2, K_1, and O_1). Tidal forcing is particularly important in the gulf, which has large tidal currents in the northern gulf around the sills of the large mid-riff islands (López *et al.*, 2021; and see Figure 1 for the location of the islands). The model has 41 vertical layers (35 at the mouth of the gulf), and a horizontal resolution of 1/12.5° which is a about an 8 km meridional increment at the mouth of the gulf. Details on the initial conditions and spin-up of the simulation; and when the tides are turned on, are given in Bujisman *et al.* (2017). The simulation comprises one year from October 1st, 2011 to September 30, 2012, and fields are available hourly. The simulation does not include data assimilation. All results presented in this article are from this HYCOM simulation.

Using the hourly fields, we calculated instantaneous zonal transport by multiplying the meridional velocity by the model's variable layer thicknesses. The model velocities are always located at the center of any existing layer, whether the layer is isopycnic (variable depth and location) or fixed water depth. We then obtained a temporal mean of the transport which was then integrated across the mouth of the gulf, and across zonal sections inside the gulf, to obtain vertical profiles of the transport. We also obtained zonal sections of vertically integrated

transport across the mouth of the gulf over the whole depth range or over certain depth ranges where there is mean inflowing or outflowing transport.

The seasonal fields were obtained by first calculating monthly averages from the hourly fields. Months were calculated starting from October 1st, 2011, but they were of equal duration (30.5 days) so that no month had more observations than other. The seasonal fit was made to a constant mean, and to annual and semiannual harmonics according to

$$Q = A_0 + A_1 cos(\omega t - \theta_1) + A_2 cos(2\omega t - \theta_2)\,.$$

The coefficients (A_0, A_1, A_2) and the phases (θ_1,θ_2) were obtained by a least square fit to the monthly data at times t; and ω represents the annual frequency. Q represents velocity or transport.

The transport at the mouth and at the interior of the gulf was obtained along zonal sections spanning the width of the gulf. The zonal section at the mouth of the gulf is shown in Figure 1. Therefore, we calculated the inflowing or outflowing meridional transports across zonal sections. However, given the time scales involved in this study (mean and seasonal), the conservation of mass implies that this meridional transport integrated across the gulf (black lines is Figure 1) is equal to the transport at the

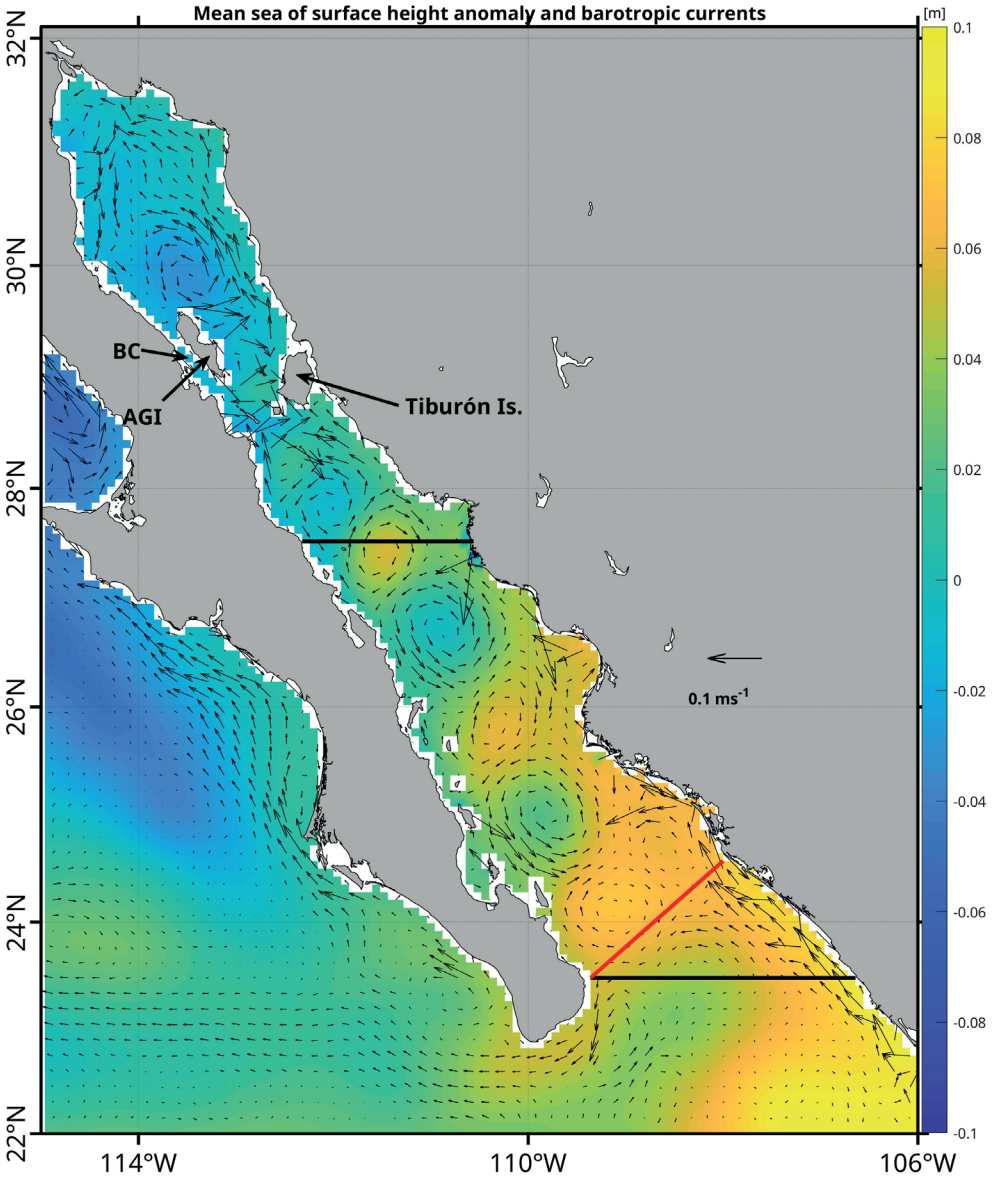

Figure 1. Modeled yearly mean sea surface height and barotropic currents in the Gulf of California. The zonal sections (black lines) across the gulf, is where vertical profiles of transport appearing in Figure 3 were calculated. The across-gulf section corresponding to the mouth of the gulf (red line) is also shown. AGI and BC stand for Ángel de la Guarda Is., and Ballenas Channel, respectively.

corresponding across-gulf (perpendicular to the axis of the gulf) section starting at the same grid point on the peninsular side of the mouth of the gulf (e.g., red line in Figure 1). Similar zonal sections were used by Zamudio *et al.* (2008, 2010, 2011) to show flow into and out of the gulf.

3. Results

3.1 Mean fields

Figure 1 shows the yearly mean of sea surface height and barotropic currents in the gulf. The most conspicuous feature is the train of eddies with alternating sense of rotation, spanning the whole length of the gulf, starting with a relatively weak anticyclonic eddy just north of the zonal section at the mouth. The eddies in several parts of the gulf have been documented in observational and modelling studies (e.g., Lavín *et al.*, 1997; Pegau *et al.*, 2002; Martínez Alcala, 2002; Zamudio *et al.*, 2008; Lavín *et al.*, 2013), but this is the first time that they have been shown to span the whole length of the gulf in a one-year mean numerical simulation. The northernmost cyclonic eddy, to the north of Ángel de la Guarda Island (see Figure 1) has been shown to reverse signs seasonally, being cyclonic in summer and anticyclonic in winter (Lavín *et al.*, 1997). The eddy in the northern gulf does reverse sign in this simulation (not shown but see Acosta-Solís, 2023) being anticyclonic in fall; cyclonic in spring and summer, and not well defined in winter. The mean, however, turns out to show a cyclonic eddy for this particular yearly simulation. Figure 1 also shows a strong Mexican coastal current (MCC) entering the gulf along the eastern coast. However, in the mean field, the MCC does not show up as a recognizable feature inside the gulf as the train of eddies dominate the mean circulation and give rise to alternating flows along the eastern coast.

The mean meridional velocity at the mouth of the gulf in the upper 500 m is shown in Figure 2. The mean velocity field

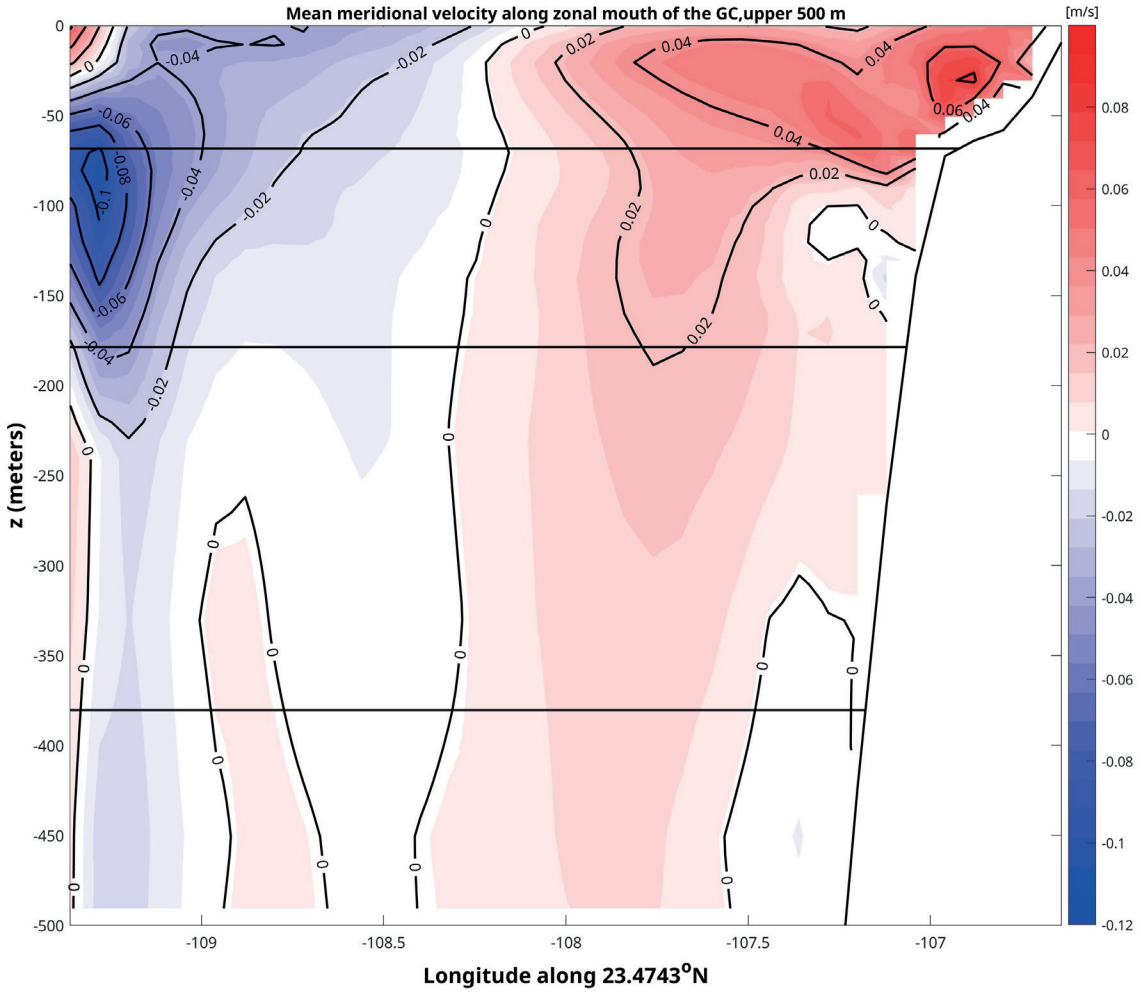

Figure 2. Modeled zonal section of the annual mean meridional velocity at the mouth of the gulf (upper 500 m). The horizontal lines are the boundaries of the first three layers in which the transport is inflowing or outflowing (see Figure 3 and Table 1). Inflow is shaded red, and outflow white and blue. Contour interval is 0.02 m/s.

is approximately evenly divided in inflow through the eastern half and outflow in the western half. The core of the outflow is deeper (~ 80 m), more intense, and localized on the western side, than the inflow on the eastern side (~ 25 m). There are, however, some smaller scale, localized flow reversals. Most notably a relatively small and intense inflow on the surface western side corner, and two weaker outflows on the eastern coast centered around 125 and 450 m. It is rather remarkable that the general, large-scale pattern of inflow and outflow in Figure 2 resembles very well the mean geostrophic velocity calculated by Collins and Castro (2022) based on 18 cruises taken on different years (see their Figure 3d). The agreement between the modeled and the observed fields includes the depth of the outflow core on the western side. The almost evenly divided outflow and inflow in the western and eastern sides, respectively, is also obtained by Collins *et al.* (1997) for four individual sections.

The laterally integrated transport at zonal sections results in a vertical profile of transport. Two profiles, one at the mouth and another one around a mid-gulf section (see Figure 1) are shown in Figure 3. At the mouth the transport is arranged in six layers of alternating inflow (at the top) and outflow layers. The same six layers are found in the mid-gulf section, but the lowest three layers have a very small transport. It is important to mention that since the values in Figure 3 are already in Sverdrups, the total transport in each of the six layers is the sum of the transports in each of the model's layers (given by the circles in Figure 3) which are inflowing or outflowing; and, therefore, the transport is not proportional to the area between the curve and the vertical axis. The values of the transport in each of the inflowing and outflowing layers, together with their standard errors and depth ranges, are given in Table 1. At the surface there is mean inflow of Pacific waters, followed below by an outflow which should include GC waters, possibly mixed with Pacific waters from below and/or above. The third inflowing layer is consistent with inflow of subsurface subtropical water from the Pacific Ocean (Castro *et al.*, 2006; Portella *et al.*, 2016). The fourth layer has a very small mean transport, and the inflowing fifth layer would be consistent with the inflow of Pacific intermediate water (Portela *et al.*, 2016). The deepest layer has a net outflowing transport, necessarily composed of Pacific deep water. Note that the

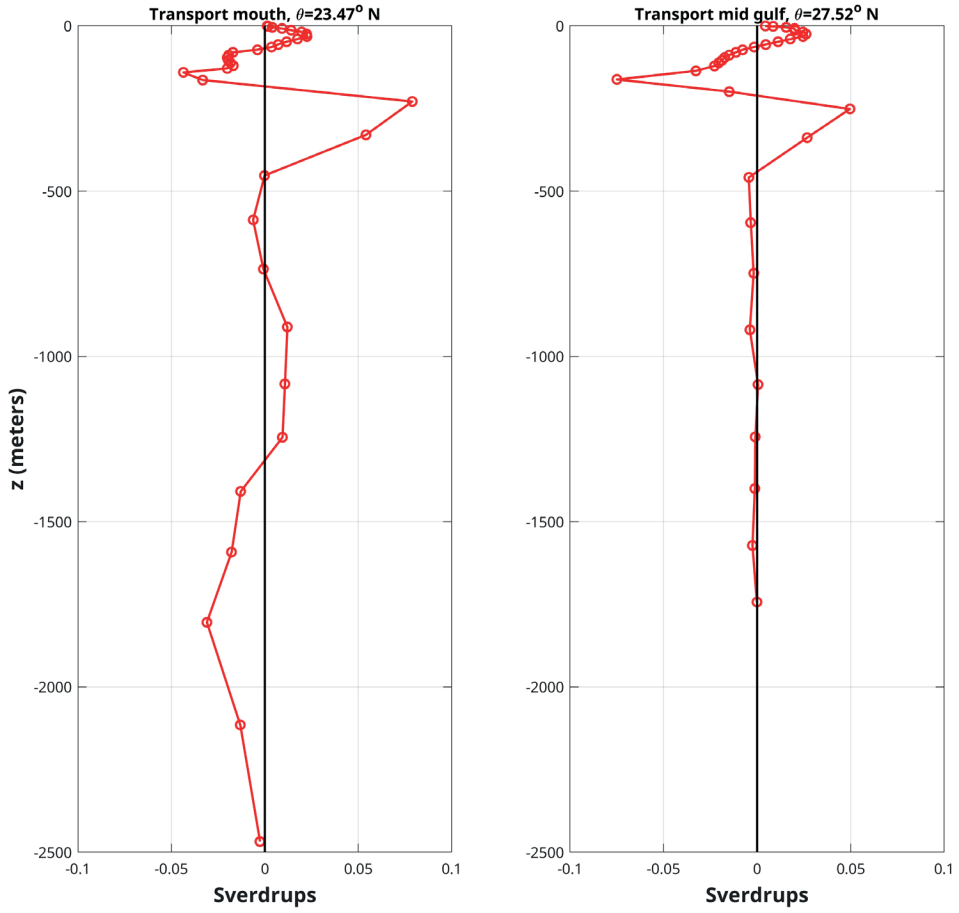

Figure 3. Modeled across-gulf integrated transport at zonal sections at the mouth of the gulf (left) and at a mid-gulf section (right). Symbols represent the transport at the model's vertical layers. Locations of the zonal sections are shown in Figure 1.

Table 1. Modeled transports in the inflowing and outflowing layers shown in Figure 3. Positive values are transport into the gulf.

	Mouth		Mid-gulf	
Layer	**Depth range (m)**	**Transport (Sv)**	**Depth range (m)**	**Transport (Sv)**
1	0 - 68	0.135 ± 0.114	0 - 59	0.177 ± 0.073
2	68 - 179	-0.213 ± 0.060	59 - 211	-0.236 ± 0.059
3	179 - 380	0.133 ± 0.070	211 - 381	0.077 ± 0.018
4	380 - 822	$-7.2 \times 10^{-3} \pm 0.11$	381 - 994	-0.012 ± 0.022
5	822 - 1325	0.032 ± 0.07	994 - 1147	$7.04 \times 10^{-4} \pm 0.007$
6	1325 - 2621	-0.077 ± 0.091	1147 - 1725	$-5.32 \times 10^{-3} \pm 0.007$

transport in the deepest layer is more than half of the transport of the surface layer, and it implies a mean downwelling from the layer above. Mean meridional velocities averaged across the zonal section are small ($\lesssim 0.01$ *m/s*, not shown) but transports are significant; for example, mean, across-gulf averaged velocities in the lowest two layers are less than 1 *mm/s*, but their transports are significant. The first four layers in the mid-gulf section have approximately the same depth ranges, and the first two have similar transports, as the corresponding ones at the mouth. The transport in the outflowing fourth layer of the mid-gulf section is significantly greater than the corresponding one at the mouth.

The annual mean, vertically integrated meridional transport at the zonal section across the mouth of the gulf is shown in Figure 4, together with the transports at each of the six inflowing and outflowing layers appearing in Figure 3 and Table 1. The bulk of the vertically integrated transport enters the gulf through half of the section on the eastern side, whereas most of the outflow takes place in a more concentrated core of larger transports next to the western side. These two inflowing and outflowing regions adjacent to the coasts are separated by two less intense bands of outflowing and inflowing transport (see Figure 4). The same general pattern of broad inflow on the eastern side and concentrated outflow in the western side is present in all six layers where the laterally integrated transport is inflowing or outflowing. Most of the inflow on the eastern side occurs in the first layer, whereas the largest concentrated outflow on the western side occurs in the second and fourth layers.

The across-gulf, integrated meridional transport *along the gulf*, down to 800 m, is shown in Figure 5, which is constructed from transport profiles as the ones appearing in Figure 3, but at all latitudes of the model. The along-gulf section is plotted to 29.76ºN. Northward of this latitude the gulf shallows significantly and the two deeper layers (roughly below 200 m) start losing their continuity, therefore it is difficult to identify inflowing and outflowing layers in the vertical. The most remarkable feature of this Figure is that the first four inflowing and outflowing layers preserve their continuity and approximate depth range, almost all of the gulf's length. In particular, the inflowing surface layer, of approximately 60 m depth, remains almost constant throughout the length of the gulf.

The meridional transport in the first layer shown in Figure 5 is shown in Figure 6. Note that the transport is everywhere positive (into the gulf) in the first layer. The difference in transport of the first layer, between the interior points and the transport at the mouth gives the average vertical transport into the first layer. Dividing the vertical transport by the gulf's area up to the interior point gives the average vertical velocity between the mouth and the interior point. This mean vertical velocity is also shown in Figure 6 and is almost everywhere positive indicating mean upwelling into the surface layer. The mean vertical velocities are small, but upwelling may be concentrated in certain areas of the gulf such as the western and eastern coasts; and in Ballenas Channel (Badan-Dangon, *et al.*, 1985; López *et al.*, 2006).

3.2 Seasonal cycles

Zonal, seasonal sections of meridional velocity at the mouth of the gulf are shown in Figure 7. Fall starts on Oct. 1st, 2011 and all seasons have the same duration (91.5 days). In general, there is surface inflow through the eastern side and surface outflow through the western side, consistent with the cyclonic circulation of the barotropic currents (Figure 1). However, there are noticeable smaller scale seasonal patterns. All year there is a localized small inflow on the surface western corner, which is largest in winter, in turn, it is this season which has the smallest exchange velocities between the gulf and the Pacific Ocean. The largest inflow is always localized in the eastern shelf. Spring and summer appear as the seasons with the largest exchange velocities, and with a strong localized subsurface core of out-

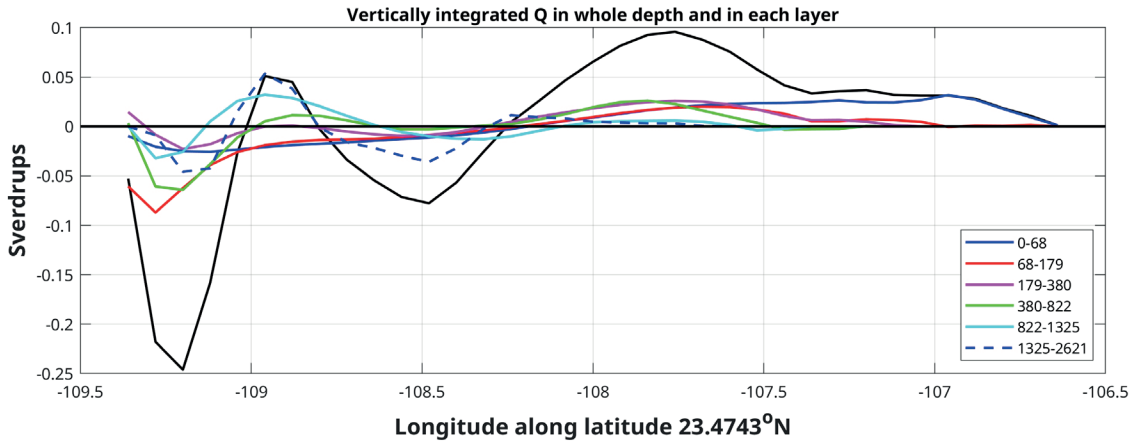

Figure 4. Modeled annual mean, vertically integrated transport across the zonal section at the mouth of the gulf (thick black line). The colored and/or dashed lines are the transports at the six different layers where there is inflow or outflow mean transport (see figure 3 and table 1). The color code of the six layers and their depth range is given in the inset.

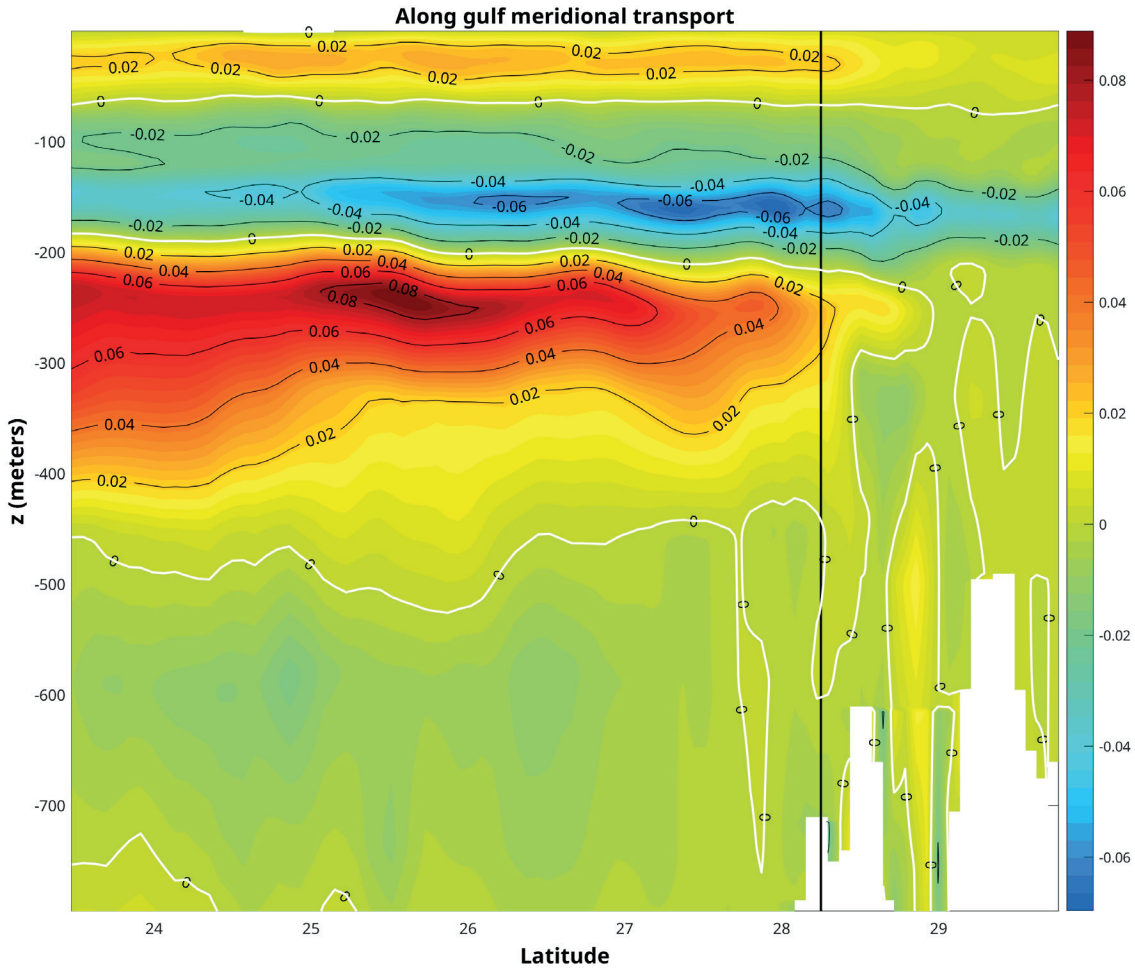

Figure 5. Modeled along-gulf, mean meridional transport integrated in zonal sections along the gulf. Contours of zero transport are white. The black vertical line marks the southernmost sill that separates the southern gulf from Ballenas channel. Contour interval is 0.02 Sv. The field has been smoothed with a three-point running mean.

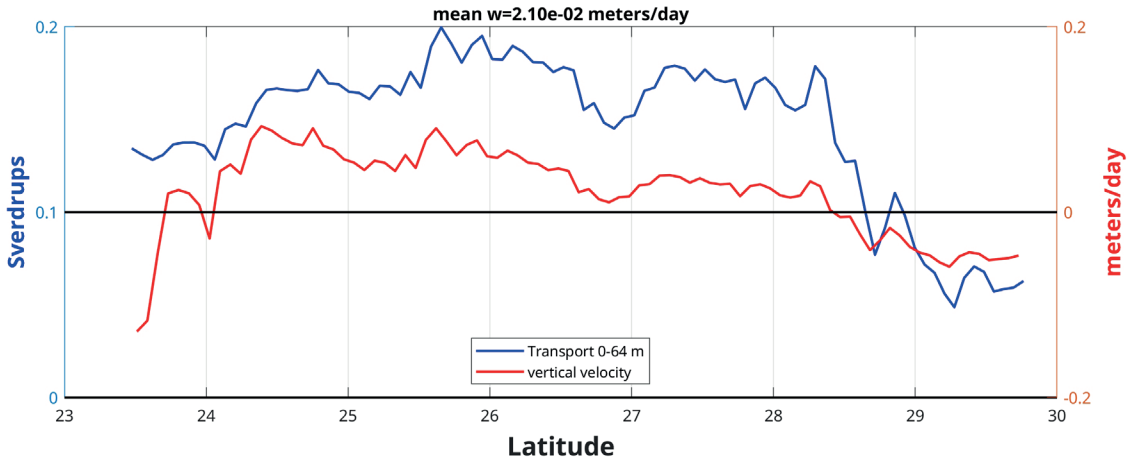

Figure 6. Modeled mean meridional transport in the zonal sections which span from the BC coast to the continental coast in the first layer (blue curve, left axis); and modeled mean vertical velocity between the given latitude and the mouth of the gulf (red curve, right axis).

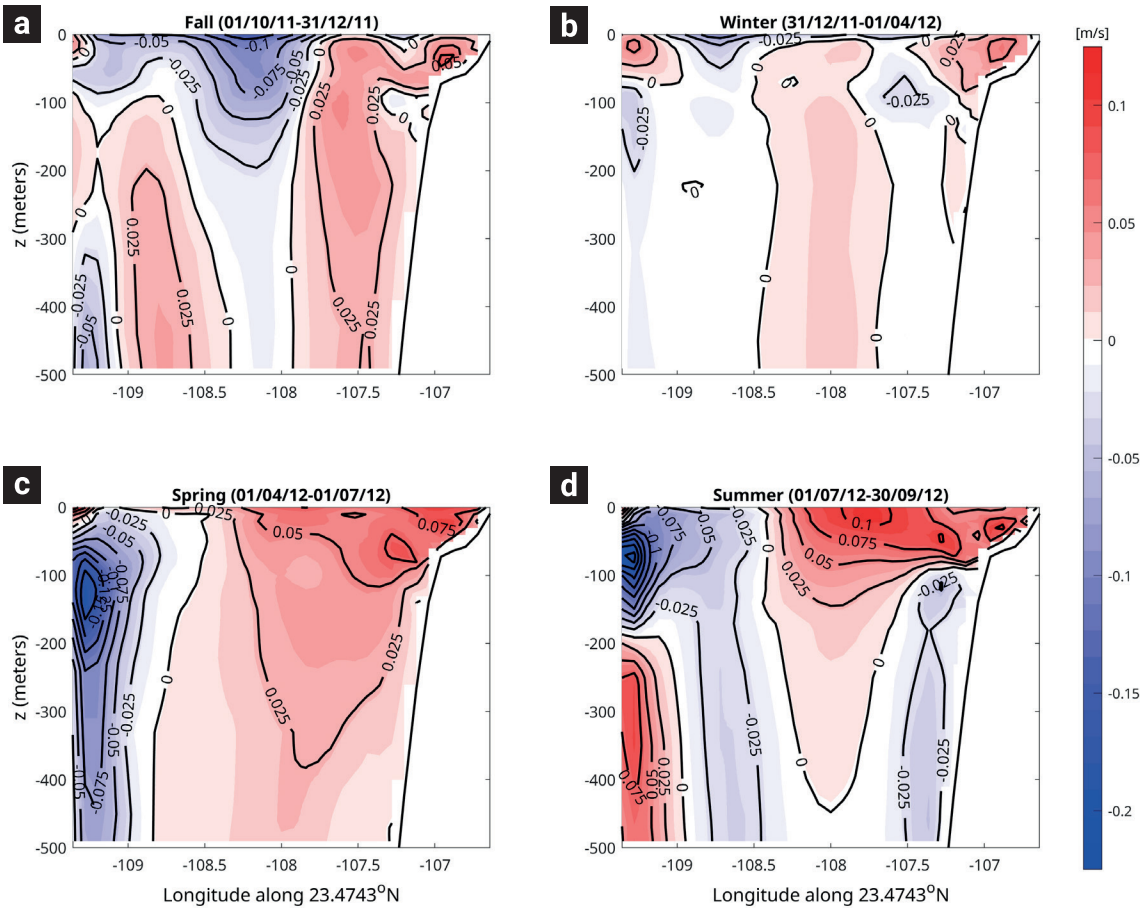

Figure 7. Modeled seasonal zonal sections of meridional velocity along the mouth of the gulf. (a) fall; (b) winter; (c) spring; and (d) summer. Inflow is shaded red, and outflow white and blue. Contour interval is 0.025 m/s.

flowing waters in the western side. Maximum, mean outflow is shifted towards the surface and away from the western coast in fall and winter.

Figure 8a shows the maximum and minimum values (including the mean) of the laterally integrated seasonal transport at the mouth, in each of the six layers appearing in Figure 3 and Table 1. The mean is also plotted to compare with the amplitudes of the seasonal cycle. In all cases the range of the seasonal cycle is larger than the mean, and, in general, they are fairly uniform (around 0.5 Sv) in the vertical, with the exception of the maximum value in layer 2 which is shifted to the left by the large negative mean value. The seasonal cycle in the second layer is essentially outflowing all year round. The largest ranges in the seasonal cycle are in layers 1 and 4. Figure 8b shows the time of the maxima, and minima of the seasonal cycle, which are separated by periods ranging from about 2.5 months (deepest layer) to 4.7 months (layer 1). The time period between minima and maxima remains almost constant at about 3.5 months between layers five to two. The time of occurrence of the minima and maxima is shifted forward in time as the year progresses from layers five to two. In the surface layer the minimum and maximum are significantly shifted in time, becoming out of phase with the layers two to five. In particular, layers one and four are 180º out of phase as can be seen in the corresponding seasonal cycles in Figure 9. Maximum inflow (outflow) in layer one (four) occurs at the beginning of summer, whereas the corresponding maximum outflow (inflow) occurs at the end of October in layer one (four). The variance explained by the seasonal fits in each layer is shown in Figure 8c. In all layers the variance explained is greater than 50%, and it is more than 80% in layers one and four. The annual and semiannual amplitudes and phases, together with their errors for all six layers are given in Table 2.

Figure 10 shows the seasonal cycle of the vertically integrated transport across the mouth of the gulf. Figure 10a is without the mean and it clearly shows a semiannual component that is dominant along most of the mouth, but most notably west of 108ºW. Maximum amplitudes are found on the western side adjacent to the coast. Figure 10b shows the same seasonal cycle as in 10a but including the mean. The pattern is very similar, but the semiannual cycle is not as evident on the eastern side. Actually, including the mean shows that the flow east of 107ºW, over the continental shelf, is into the gulf all year round, and the maximum outflow cores on the western side are more pronounced. At the western side there is outflow from mid-autumn to mid-winter, and

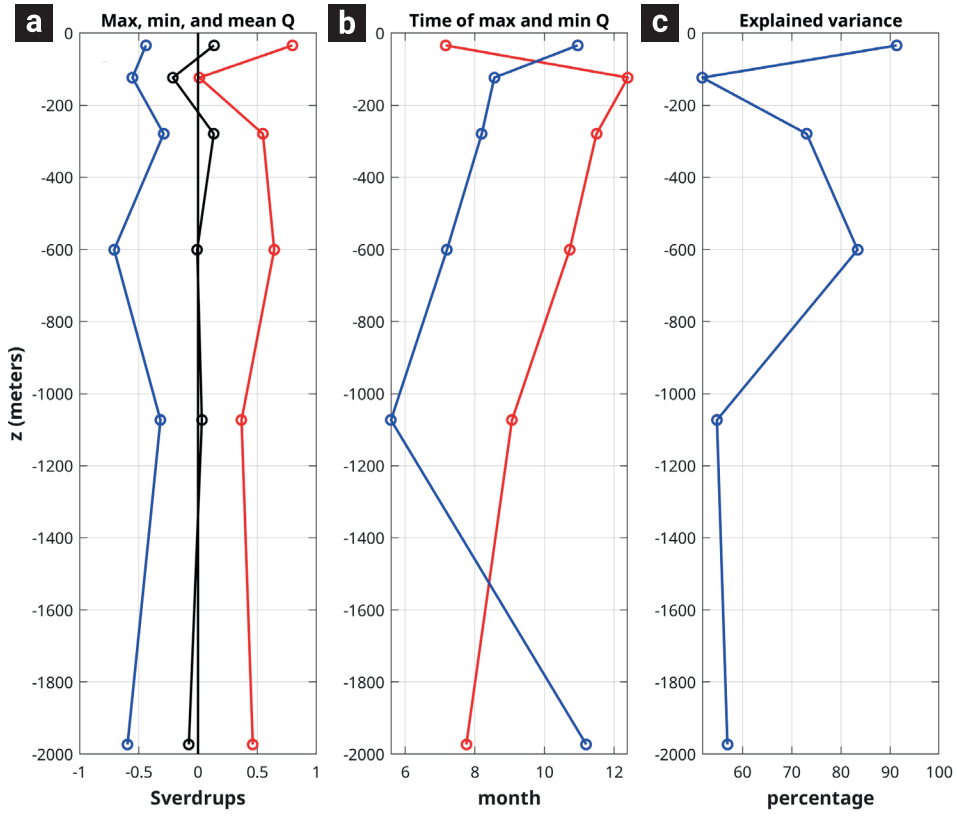

Figure 8. (a) Vertical profiles of the minima and maxima of the seasonal cycle (including the mean) and the mean (black line) of the layers appearing in Table 1 and Figure 3 at the mouth. (b) Time of occurrence along the year of the minima (blue line) and maxima (red line) of the seasonal cycle corresponding to (a). January 1st corresponds to 1.0. (c) Variance explained by the seasonal fits. All results are from the model.

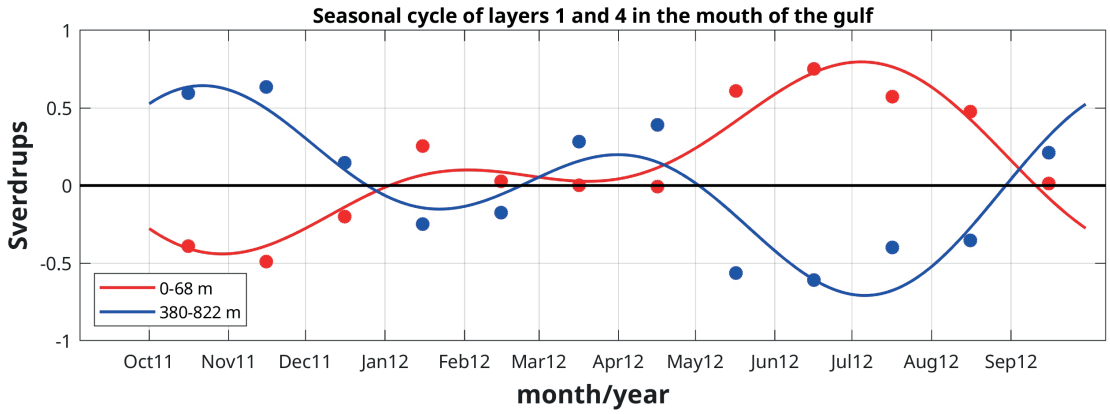

Figure 9. Modeled seasonal cycles of the transports in the surface layer (layer one, red line) and in layer four (blue line) at the mouth of the gulf. The monthly means are shown as dots with the same color as the corresponding seasonal cycles. The depth ranges of the layers are shown in the inset. Tick marks at the beginning of the month.

Table 2. Annual and semiannual amplitudes, phases and their corresponding errors for the transport in layers 1 to 6. Errors for amplitude are given in percentage of the amplitude and for phases in days.

Layer	Annual amplitude (Sv)	Error (%)	Annual phase (day/month)	Error (days)	Semiannual amplitude (Sv)	Error (%)	Semiannual phase (day/month)	Error (days)
1	0.44	14	9/6	8	0.28	21	15/7	12
2	0.21	43	5/2	25	0.13	69	21/11	40
3	0.14	56	28/12	32	0.32	25	10/11	15
4	0.36	25	3/12	15	0.41	23	12/10	13
5	0.18	53	13/10	31	0.21	46	25/8	26
6	0.26	53	17/6	31	0.33	42	30/7	24

from mid-spring to mid-summer, and inflow during mid-winter to mid-spring, and from mid-summer to mid-autumn. The outflow and inflow maxima on the western side, occur earlier in the year as one moves east, and there appears to be a westward propagation pattern west of 108ºW which we have emphasized by drawing a sloping line in Figure 10a.

Figure 11 shows plots similar to Figure 10, but for layers 1 and 4 (see Table 1), both including the mean. In both layers, there is a strong semiannual component on the western side close to the coast (west of 109ºW) where localized cores of inflow and outflow alternate throughout the year. Plots, similar to the ones in Figure 11 but for the other 4 layers (not shown), show that the semiannual component on the western side is present at all depths. In layer 1, there is inflow almost in the entire section (east of 109ºW) during late spring and summer; and all year east of 107ºW, consistent with Figures 7 and 10. The rest of the year, at the mouth, there are regions of inflow and outflow in most of the section. In layer four (Figure 11b), the semiannual component is present in most of the section, which is consistent with the amplitudes of the annual and semiannual component for this layer (see Table 2). Note that in layer 4 there is clear evidence of western propagation at the semiannual frequency west of about 108ºW, however there is no similar evidence in layer 1. Actually, there is only evidence of western propagation in layers three to six which does show up when vertically integrating all six layers from surface to bottom (Figure 10). Note also, that on the western side, where there is a clear semiannual component, layers one and four are not quite 180º out of phase, they are more like 90º out of phase. However, when integrated across the mouth of the gulf they do become 180º out of phase and are dominated mainly by the annual frequency (see Figure 9).

The seasonal cycle of the mean across-gulf averaged transport *along the gulf* in the first layer is shown in Figure 12. As is evident in the mouth (Figure 9), the transport in the interior of the gulf in the first layer, has a predominant annual frequency and is practically in phase all along the gulf. Including the mean,

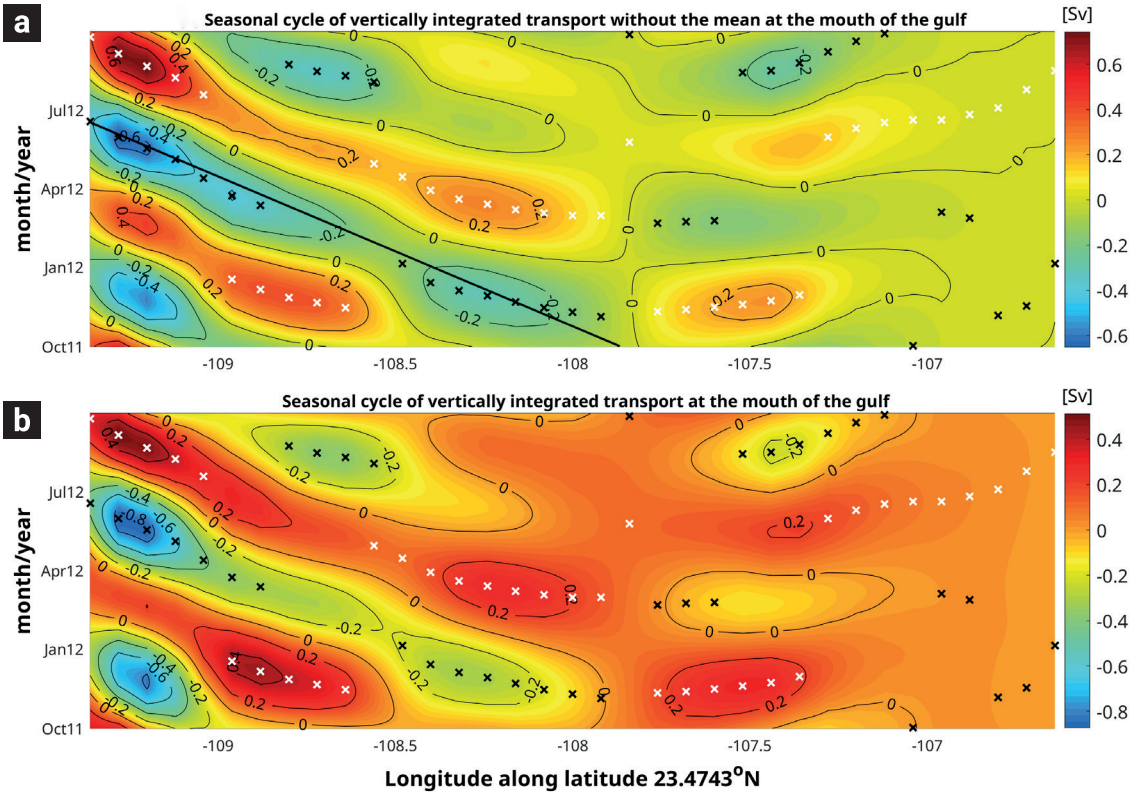

Figure 10. (a) Modeled seasonal cycle, without the mean, of the vertically integrated transport along the zonal mouth of the gulf. (b) As in (a) but including the mean. White (black) crosses mark the maximum (minimum) at each location along the mouth. Contour interval is 0.02 Sv.

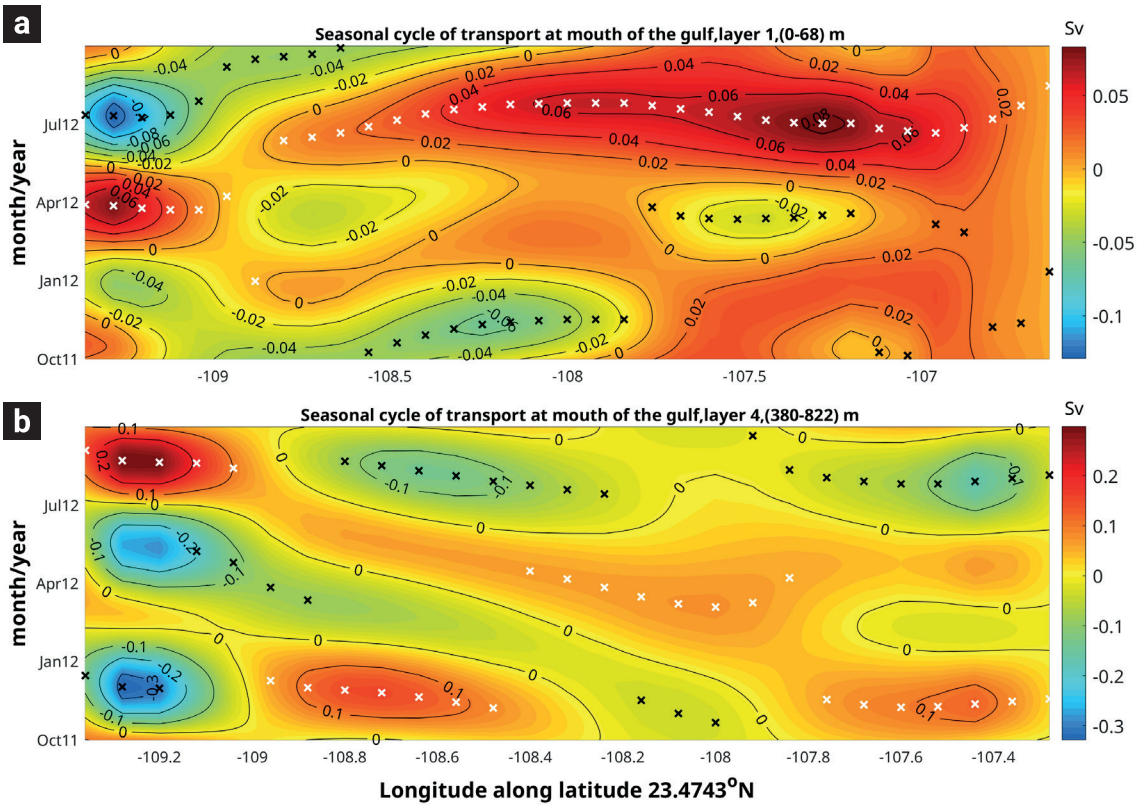

Figure 11. (a) Modeled seasonal cycle (including the mean) of the vertically integrated transport along the zonal mouth of the gulf in layer 1(0-68 m). (b) As in (a) but for layer 4 (380-822 m). White and black crosses are as in Figure 10. Contour interval is 0.02 (0.01) Sv in (a) ((b)).

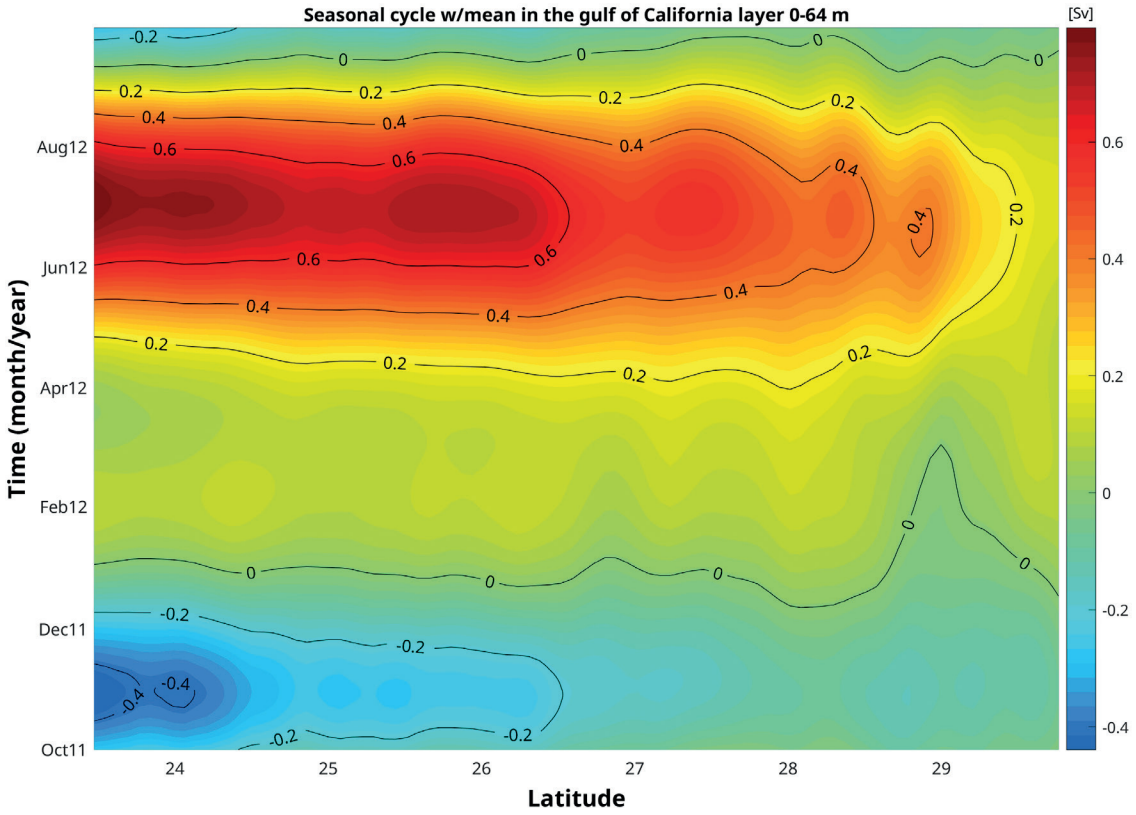

Figure 12. Modeled seasonal cycle (including the mean) of the laterally integrated transport along the gulf in the first layer. The field has been smoothed with a three-point running mean. The contour interval is 0.2 Sv.

there is outflow only during the fall (September to December) and inflow the rest of the year. The largest outflow occurs during the end of October and the largest inflow at the beginning of summer. The largest inflow and outflow occurs at the mouth, with a secondary smaller maximum inflow around 26ºN. Northward of this latitude, inflow and outflow decrease towards the head of the gulf. In the second layer, the seasonal cycle including the mean (Figure 13), shows that, practically all along the gulf, there is outflow, with small pockets of very weak inflow during the end of the fall. There appears to be a small phase shift in the maximum outflow during mid-summer, with maximum outflow occurring earlier in the interior of the gulf. Note that the along-gulf extent of the second layer is smaller than for the first layer because the second layer losses its continuity around 28.5ºN (see Figure 5).

4. Discussion and Concluding Remarks

Unfortunately, there are not many observations which we can compare with, especially since transport averaged across the gulf is difficult to estimate from observations. However, there is very good agreement with the three layer, near-surface (0-500 m) circulation found by Bray (1988) in the mid-gulf section using geostrophic velocities based on data from several years. As we did with the model, Bray also found an outflowing subsurface layer (50-250 m) and an inflowing layer from 250 m down to 500 m. For the surface layer, Bray (1988) did not establish a mean transport but only stated that it reverses with the seasonal winds, flowing towards the head in summer and towards the mouth in winter. Here we have shown that, in the model, the net transport in the surface layer is northward and, therefore, into the gulf, and that there is a seasonal flow reversal, but with the transport flowing most of the year into the gulf, and only out of the gulf during fall (Figures 9, and 12). The phase of the transport in the surface layer (the transport is essentially in phase all along the gulf) also agrees rather remarkably well with the phases of surface geostrophic velocities estimated by Ripa and Marinone (1989), Ripa (1990) and Navarro *et al.* (2016, see their fig. 6b) with maximum inflow and outflow in summer and fall, respectively. Ripa (1997) only considered the annual frequency, but the annual fit to the observations and the associated Kelvin wave model, also have a maximum inflow of the mean surface velocity in the summer. We have also found that this three-layer, near-surface, mean circulation extends most of the gulf's length starting at the mouth (Figure 5). The mean winds are towards the

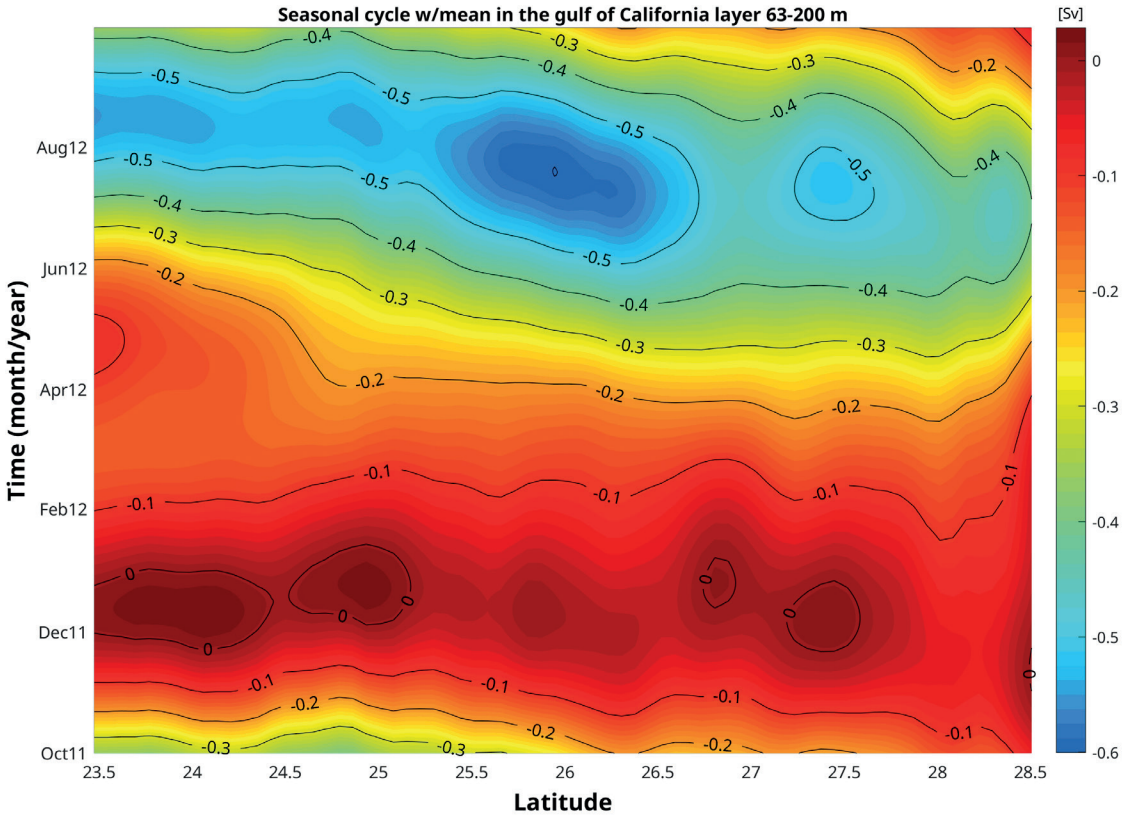

Figure 13. As in Figure 12 but for the second layer. Contour interval is 0.1 Sv.

mouth (Bordoni *et al.*, 2004), which is coincident with the mean winds used to force the HYCOM (not shown). However, the mean transport in the surface layer is towards the north, contrary to the mean winds. Furthermore, the seasonal cycle of the winds shows that they only flow towards the north in summer and towards the south the rest of the year (Bordoni *et al.*, 2004; Collins and Castro, 2022). Therefore, the mean and seasonal transport of the surface layer does not appear to be directly forced by the local winds, highlighting the role of the eastern tropical Pacific Ocean in the circulation of the gulf, which also has been found to be important in the coastal circulation along the western Mexican coast (Gómez-Valdivia *et al.*, 2015).

We have already mentioned the good agreement between Figure 2 and the corresponding Figure 3d in Collins and Castro (2022). These authors, also calculated the across-gulf integrated transport at the mouth of the gulf in the upper 400 m. They also have an inflowing surface layer down to about 150 m, and an outflowing layer from 150 m down to 400 m, but there is not an inflowing third layer, at least down to 400 m. We also found a general qualitative agreement between Figure 2 and a corresponding seven-year mean, modeled velocity by Zamudio *et al.* (2008). There are, however, some important differences. Most notably, they do not obtain the small surface inflow on the western side, their western outflow core is not adjacent to the coast and it is surface intensified; and their subsurface, eastern outflow region is somewhat larger. Some of these differences may be due to the fact that they computed a seven-year mean, as compared to just one year in here; but some differences may also stem from the smaller vertical resolution they used (20 layers).

The Mexican Coastal Current (MCC) is a subsurface poleward flow adjacent to the west coast of Mexico. At ~17°N the current also flows at the surface and reaches the mouth of the gulf (Kessler, 2006; Lavín *et al.*, 2006; Godínez *et al.*, 2010; Gómez-Valdivia *et al.*, 2015; Portela *et al.*, 2016). Figure 2 is consistent with the poleward flow in the eastern part of the section. The poleward flow through the eastern side is present in the first three layers where the mean transport flows in alternating directions (Figures 2 and 4), but the across-gulf integrated transport in the second layer is equatorward (Figure 3 and Table 1). Therefore, in the second layer, the transport coming out from the gulf is larger than the inflowing transport from the MCC. The outflow in the second layer is concentrated in a subsurface core centered at ~100 m which is stronger and more concentrated than the shallower poleward flow over the continental shelf on the eastern side (Figure 2).

The seasonal variation of the MCC is poorly known. Kessler (2006) and Portela *et al.* (2016) identified the strongest poleward flow reaching the gulf in summer. Gómez-Valdivia *et al.* (2015), using a numerical model, found a semiannual variation of the current with maxima in spring and fall, associated to the arrival of coastally trapped waves from the equator. Figure 7 shows that there is poleward flow through the eastern part of the gulf all year round, with largest velocities in summer and smallest in winter. Assuming that the MCC at the gulf's entrance covers layers one, two, and, possibly, part of the third (Table 1), then Figure 10 and Figure 11a, and similar figures for layers 2 and 3 (not shown), show that there is, indeed, a strong semiannual signal, although concentrated more on the western side of the mouth of the gulf. On the eastern side, where the MCC flows into the gulf, there is a significant contribution from the semiannual harmonic with the greatest inflow in summer and the greatest outflow in spring. There are smaller maxima and minima in winter and fall, respectively, which are more evident in the combined seasonal cycle of layers 1 and 2 (not shown).

Figures 10 and 11b strongly suggest a westward propagation west of 108ºW at the mouth of the GC, which is highlighted by the sloping black line in Figure 10a. The slope of that line gives a very small propagation speed of 0.7 cm/s. To see if this could correspond to a Rossby wave of semiannual frequency, we calculated the parameters of such a wave. The critical (minimum) period of a Rossby wave depends on latitude and coastal orientation (Clarke and Shi, 1991). Around the mouth of the gulf, Clarke and Shi (1991) calculated two very different critical periods of 172.4 and 260.3 days. To allow for the propagation of the semiannual frequency we will take the lower critical period which corresponds to an almost meridional coastline. For that period, the internal radius of deformation can be obtained from the expression of the maximum critical frequency of Rossby waves for a meridional coastline, namely $a=2\omega_c/\beta$, where ω_c, corresponds to the critical frequency (*i.e.*, the frequency corresponding to the critical period of 172.4 days), and β is the meridional gradient of the Coriolis parameter. Taking the value of β at the mouth of the gulf gives $a=40.2$ *km*, which corresponds to a first mode, internal gravity wave propagation speed of 2.33 *m/s*. With the value of a we can calculate the wavelengths and phase speeds of the corresponding long, and short, purely westward (phase propagation) Rossby waves at the semiannual frequency. The values are 355.5 km and phase speed of 2.3 cm/s for the long wave, and 179.2 km and phase speed of 1.1 cm/s, for the short wave. For the phase speed of 0.7 cm/s inferred from Figure 10a, the corresponding wavelength for the semiannual frequency is 110.4 km. Therefore, the propagating pattern in Figures 10 and 11, corresponds much more closely to the short Rossby wave, and given the uncertainties in the values of the Rossby radius of deformation, and in the empirical estimation of the phase speed from Figure 10a, this seems like a reasonable approximation.

The calculation of the net outflowing, laterally integrated transport, enables us to estimate a lower bound for the turnover time of the gulf (Talley *et al.*, 2011). The net outflowing transport is essentially the same as the inflowing transport, the small difference being the water evaporated in the gulf. From Table 1, the sum of the outflowing transport is 0.2972 *Sv*. The volume of the gulf delimited by the zonal mouth used in this work, is $1.3119\times10^{14}\mathrm{m}^3$. Dividing the volume by the outflowing transport gives a lower bound for the turnover time of approximately 14 years.

We have estimated the laterally integrated transport across the mouth of the gulf, and all the way to the bottom using a global, one-year simulation of the HYCOM. Using a global model ensures that the effects of the Pacific Ocean on the gulf are incorporated. The transport of the three upper layers compares qualitatively well with the limited available observations. The same upper three layers found at the mouth, are present in almost all the length of the gulf, with approximately the same thickness. The transport in the surface layer inside the gulf is almost everywhere greater than the one at the mouth, producing mean upwelling into the surface layer. This upwelling may explain the biologically rich waters of the gulf. In the surface layers, there is a concentrated outflow on the western side of the mouth of the gulf, and a broader inflow on the eastern side. The greatest seasonal exchange of the gulf with the Pacific Ocean above 820 meters occurs in summer and fall, with outflow in summer and inflow in fall, except for the surface layer where inflow and outflow are reversed with respect to the layers below. We have found that there is a strong semiannual signal in the seasonal variation of the transport, with a stronger semiannual signal concentrated in the western outflow. In the deeper layers (below 380 m) the semiannual signal on the western side is consistent with the propagation of a short Rossby wave. From the results of this work, we have left some unanswered questions which lie outside the scope of this article. More significantly, we have not addressed the causes of the water exchange found in the model, and the origins of the possible Rossby wave, both of which probably involve dynamics of the equatorial and eastern Pacific Ocean, which are left for future research.

5. Acknowledgments

This work was partially funded through a graduate scholarship granted to Gonzalo Acosta-Solís by CONAHCyT. The HYCOM simulation was performed at the Navy Department of Defense (DoD) Supercomputing Resources at Stennis Space

Center, Mississippi, using grants of computer time from the DoD High Performance Computing Modernization Program. The comments by the two anonymous reviewers improved the manuscript.

6. References

Acosta-Solís, G. (2023). El Golfo de California visto a través del modelo numérico Global HYCOM. [Tesis de Maestría]. Repositorio CICESE. **https://cicese.repositorioinstitucional.mx/jspui/handle/1007/3830**

Badan-Dangon, A., & C. J. Koblinsky, and T. Baumgartner (1985). Spring and summer in the Gulf of California: Observations of surface thermal patterns. Oceanol. Acta, 8, 1.

Baumgartner, T. R., & N. Christiensen (1985). Coupling of the Gulf of California to large-scale interannual climatic variability. *Journal of Marine Research*, 43(4), 825-848.

Beron-Vera, F. P., & Pedro Ripa (2000). Three-dimensional aspects of the seasonal heat balance in the Gulf of California. *Journal of Geophysical Research*, 105(C5), 11441-11457. doi: **https://doi.org/10.1029/2000JC900038**

Bordoni, S., P. E. Ciesielski, R. H. Johnson, B. D. McNoldy, & B. Stevens (2004). The low-level circulation of the North American Monsoon as revealed by QuikSCAT. *Geophysical Research Letters*, 31(10), L10109. doi: **https://doi.org/10.1029/2004GL020009**

Bray, N. A. (1988). Thermohaline Circulation in the Gulf of California. *Journal of Geophysical Research*. Oceans, 93(C5), 4993-5020. doi: **https://doi.org/10.1029/JC093iC05p04993**

Buijsman, M. C., B. K. Arbic, J. G. Richman, J. F. Shriver, A. J. Wallcraft, & L. Zamudio (2017). Semidiurnal internal tide incoherence in the equatorial Pacific, *Journal of Geophysical Research*. Oceans, 122(7), 5286–5305. doi: **https://doi.org/10.1002/2016JC012590**

Castro, R., C. A. Collins, T. A. Rago, T. Margolina, & L. F. Navarro-Olache (2017). Currents, transport, and thermohaline variability at the entrance to the Gulf of California (19–21 April 2013). *Ciencias Marinas*, 43(3). doi: **https://doi.org/10.7773/cm.v43i3.2771**

Castro, R., M. Lavín, & P. Ripa (1994). Seasonal heat balance in the Gulf of California. *Journal of Geophysical Research*. Oceans, 99(C2), 3249–3261. doi: **https://doi.org/10.1029/93JC02861**

Castro, R., Reginaldo Durazo, Affonso Mascarenhas, Curtis A. Collins, & A. Trasviña (2006). Thermohaline variability and geostrophic circulation in the southern portion of the Gulf of California. *Deep Sea Research Part I: Oceanographic Research Papers*, 53(1), 188-200. doi: **https://doi.org/10.1016/j.dsr.2005.09.010**

Clarke, A.J., & Shi, C (1991). Critical frequencies at ocean boundaries. *Journal of Geophysical Research Oceans*, 96(C6). doi: **https://doi.org/10.1029/91JC00933**

Collins, C.A., & R. Castro (2022). Observations of the exchange of ocean waters between the Pacific Ocean and the Gulf of California. *Ocean and Coastal Res*, 70(1), e22040. doi: **http://doi.org/10.1590/2675-2824070.22036cac**

Collins, C.A., Garfield, N., Mascarenhas Jr. A.S. and Sperman, M.G. (1997). Ocean current across the entrance to the Gulf of California. *Journal of Geophysical Research Oceans* 102(C9). doi: **https://doi.org/10.1029/97JC01302**

Godínez, V. M., E. Beier, M. F. Lavín, and J. A. Kurczyn (2010). Circulation at the entrance of the Gulf of California from satellite altimeter and hydrographic observations, *Journal Geophysical Research Oceans*, 115(C4), 007, doi: **https://doi.org/10.1029/2009JC005705**

Gómez-Valdivia, F., A. Parés-Sierra, & A.L. Flores-Morales (2015). The Mexican Coastal Current: A subsurface seasonal bridge that connects the tropical and subtropical Northeastern Pacific. *Continental Shelf Research*, 110, 100–107. doi: **https://doi.org/10.1016/j.csr.2015.10.010**

Kessler, W. S. (2006). The circulation of the eastern tropical Pacific: A review. *Progress in Oceanography*. 69(2-4), 181–217. doi: **https://doi.org/10.1016/j.pocean.2006.03.009**

Lavín, M. F., & S. G. Marinone. (2003). An Overview of the Physical Oceanography of the Gulf of California. In O.U. Velasco, J. Sheinbaum & J. Ochoa (Eds) *Nonlinear Processes in Geophysical Fluid Dynamics*. (pp. 173-204). Springer Dordrecht.

Lavín, M. F., E. Beier, J. Gómez-Valdés, V. M. Godínez, and J. García (2006). On the summer poleward coastal current off SW México, *Geophysical Research Letters*, 33(2), L02601, doi: **https://doi.org/10.1029/2005GL024686**

Lavín, M. F., R. Durazo., E. Palacios., M.L. Argote, & L. Carrillo (1997). Lagrangian observations of the circulation in the northern Gulf of California. *Journal of Physical Oceanography*, 27(10), 2298-2305. doi: **https://doi.org/10.1175/1520-0485(1997)027<2298:LOOTCI>2.0.CO;2**

Lavín, M. F., R. Castro, E. Beier, & V.M. Godínez (2013), Mesoscale eddies in the southern Gulf of California during summer: Characteristics and interaction with the wind stress, *Journal of Geophysical Research Oceans*, 118(3), 1367-1381, doi: **https://doi.org/10.1002/jgrc.20132**

López, M., J. Candela, & M. L. Argote (2006). Why does Ballenas Channel have the coldest SST in the Northern Gulf of California? *Geophysical Research Letters*, 33(11), L11603. doi: **https://doi.org/10.1029/2006GL025908**

López, M., L. Flores-Mateos, & J. Candela (2021). Tidal currents at the sills of the Northern Gulf of California. *Cont. Shelf Res.*, 227, doi: **https://doi.org/10.1016/j.csr.2021.104513**

Marinone, S. G. (1997). Tidal residual currents in the Gulf of California: Is the M2 tidal constituent sufficient to induce them? *Journal of Geophysical Research Oceans*, 102(C4), 8611-8623. doi: **https://doi.org/10.1029/96JC03835**

Martínez Alcala, Jose Antonio (2002), Modeling studies of mesoscale circulation in the Gulf of California. [Tesis de Doctorado]. Oregon State University.

Mascarenhas Jr., A. S., R. Castro, C. A. Collins, & R. Durazo (2004). Seasonal variation of geostrophic velocity and heat flux at the entrance to the Gulf of California, Mexico. *Journal of Geophysical Research*

Oceans, 109(C07). doi: **https://doi.org/10.1029/2003JC002124**

Navarro, R., M. Lopez, and J. Candela (2016), Seasonal cycle of near-bottom transport and currents in the northern Gulf of California, *Journal of Geophysical Research Oceans*, 121(12), 8621–8634, doi: **https://doi.org/10.1002/2016JC012063**

Pegau, W. S., E. Boss, & A. Martínez (2002). Ocean color observations of eddies during the summer in the Gulf of California. *Geophysical Research Letters*, 29(9). doi: **https://doi.org/10.1029/2001GL014076**

Portela E. *et al.* (2016). Water Masses and Circulation in the Tropical Pacific off Central Mexico and Surrounding Areas. *Journal of Physical Oceanography*, 46(10), 3069-3081. doi: **https://doi.org/10.1175/JPO-D-16-0068.1**

Ripa, P. (1990), Seasonal circulation in the Gulf of California, Ann. Geophys., 8(7-8), 559–564.

Ripa, P. (1997). Towards a physical explanation of the seasonal dynamics and thermodynamics of the Gulf of California. *Journal of Physical Oceanography*, 27(5), 597–614. doi: **https://doi.org/10.1175/1520-0485(1997)027<0597:TAPEOT>2.0.CO;2**

Ripa, P., and S. G. Marinone (1989), Seasonal variability of temperature, salinity, velocity, vorticity and sea level in the central Gulf of California, as inferred from historical data, Quarterly Journal of the Royal Meteorological Society, 115(488), 887-913. doi: **https://doi.org/10.1002/qj.49711548807**

Talley, L.D., G.L. Pickard, W.J. Emery, & J.H. Swift (2011). *Descriptive Physical Oceanography*, Sixth Ed. Academic Press. doi: **https://doi.org/10.1016/C2009-0-24322-4**

Zamudio, L., E. J. Metzger, & P. Hogan (2011). Modeling the seasonal and interannual variability of the northern Gulf of California salinity, *Journal of Geophysical Research Oceans*, 116(C2). doi: **https://doi.org/10.1029/2010JC006631**

Zamudio, L., E. J. Metzger, & P. J. Hogan (2010). Gulf of California response to Hurricane Juliette. *Ocean Modelling*, 33(1-2), 20-32. doi: **https://doi.org/10.1016/j.ocemod.2009.11.005**

Zamudio, L., P. Hogan, & E. J/ Metzger (2008). Summer generation of the Southern Gulf of California eddy train. *Journal of Geophysical Research*, 113(C6). doi: **https://doi.org/10.1029/2007JC004467**